Functional Materials

DOI: 10.1002/anie.201107216

# $SiO_2$-Surface-Assisted Controllable Synthesis of TaON and $Ta_3N_5$ Nanoparticles for Alkene Epoxidation**

*Qingsheng Gao,* Sinong Wang, Yuchun Ma, Yi Tang, Cristina Giordano, and Markus Antonietti*

Metal nitrides are promising materials because of their prominent properties originating from metal–nitrogen bonds and noble-metal-like electron features, such as thermal stability, mechanical hardness, superconductivity, and high catalytic performance in hydrocarbon conversion.[1] More importantly, their bulk and surface properties are significantly associated with the nitridation levels, which can be adjusted as such. Taking tantalum (oxy)nitrides as the current example, introducing N atoms into $Ta_2O_5$ brings a remarkably narrowed and tunable band-gap energy, thus enabling novel visible-light photocatalysts.[2] Meanwhile, the catalytic properties of Ta in tantalum (oxy)nitrides for nonphotocatalytic reactions are also expected to be improved because of the tailored nitridation and easier electron transfer from N (vs. O) to Ta centers. However, there are still no reports on these effects to the best of our knowledge. Significantly, such modulation of material properties by controlled nitridation provides a new strategy for designing novel catalysts.[2a,3]

The controllable synthesis of TaON and $Ta_3N_5$ nanoparticles (NPs) with tailored chemical composition is therefore an attractive goal,[2e,3a] which is, however, difficult to achieve by current strategies because of easy overreactions of nitridation.[4] For example, by-products of $Ta_3N_5$, $Ta_4N_5$, and even TaN will be easily generated from further nitridation of TaON during calcination. The traditional method using $NH_3$ is limited for the danger associated with using $NH_3$ at high temperature and the complexity related to the rigid control of gas composition, flow rate, and pressure.[4,5] Moreover, although urea and cyanamide have been reported as safe nitrogen sources for preparing tantalum nitrides, only impure and deeply reduced TaN could be obtained, as an effective control on reactions is absent.[6]

Recently, we discovered that the controlled release of N source from urea is significant to control metal nitridation.[7] As a further controlled version of urea pyrolysis, we present herein a new $SiO_2$-surface-assisted strategy for the controlled fabrication of TaON and $Ta_3N_5$ NPs, which successfully avoids the disadvantage mentioned above. Assisted by $SiO_2$, the production of TaON over $Ta_3N_5$ NPs with tailored composition was achieved through calcination of Ta–urea (TaU) gels with suitable urea/Ta ratios ($R_{U/Ta}$). A mechanism is proposed that urea is converted into carbon–nitride ($CN_x$) species on $SiO_2$-surface at mild temperature,[8] which further acts as a slow release N source for controlled nitridation. The electronic properties of Ta are tuned by the different nitridation levels in TaON and $Ta_3N_5$ NPs, which significantly improves the activity for alkene epoxidation, as compared to $Ta_2O_5$ NPs. This is the first time to discover that introducing N into $Ta_2O_5$ can remarkably improve epoxidation activity because of the easier electron transfer from N (vs. O) to Ta. Furthermore, the controlled nitridation endows catalysts with tunable surface basicity, noticeably influencing epoxidation selectivity. Owing to the facile synthesis and prominent catalytic behavior associated with tailored nitridation, we believe that our effort will pave the way for designing nanostructured catalysts of metal–nitrides.

As the key assisting agent, $SiO_2$ NPs (5–15 nm, $S_{BET} = 527.3\ m^2 g^{-1}$) were added into TaU precursor, resulting in a homogenous gel denoted as TaU/SN. After calcination under $N_2$ flow and following treatment with NaOH solution, highly crystalline TaON and $Ta_3N_5$ NPs were obtained at $R_{U/Ta}$ values of 1.5 and 3.0, respectively. These products were confirmed as γ-TaON (ICDD: 01-076-3258) and $Ta_3N_5$ (ICDD: 04-004-4564) by their X-ray diffraction (XRD) patterns (Figure 1 a). Scanning electron microscopy (SEM) and transmission electron microscopy (TEM) images (Figure 1 b–e) show that the products are NPs with size of 20–25 nm, which can be easily dispersed in EtOH or water by ultrasonic agitation. The size nicely fits with the calculated results from XRD analysis, which reveal values of approximately 20.6 nm for TaON and 18.9 nm for $Ta_3N_5$. γ-TaON can be well identified in high-resolution TEM images (Figure 1 c) by the clear lattice fringes of (110) and (001), while for $Ta_3N_5$ the planes of (200) and (110) are well observed (Figure 1 e).

The colors of samples give further clear evidence about their structures, as yellow TaON and red $Ta_3N_5$ NPs show absorption bands around 500 and 600 nm, respectively, in UV/Vis spectra (Figure S1 in the Supporting Information). This result proves the narrowing of the band gap compared with $Ta_2O_5$ as a result of nitridation. Moreover, NPs composed of tunable TaON and $Ta_3N_5$ phases are easily obtained (Figure S2) by switching the $R_{U/Ta}$ value from 1.5 to 3.0, further indicating the potential for their controlled synthesis.

Several control experiments were carried out to examine the mechanism underlying the controllable synthesis of TaON

---

[*] Dr. Q. S. Gao, Dr. C. Giordano, Prof. M. Antonietti
Department of Colloid Chemistry
Max Planck Institute of Colloids and Interfaces
Research Campus Golm, 14424 Potsdam (Germany)
E-mail: qingsheng.gao@mpikg.mpg.de

S. N. Wang, Dr. Y. C. Ma, Prof. Y. Tang
Department of Chemistry and Shanghai Key Laboratory of Molecular Catalysis and Innovative Materials
Fudan University, Shanghai 200433 (P.R. China)

[**] We thank the Max Planck Society, BMBF (035F0353A-E), the National Science Foundation of China (20873028, 21073041), and the Major State Basic Research Development Program (2009CB623506) for financial support.

Supporting information for this article is available on the WWW under http://dx.doi.org/10.1002/anie.201107216.

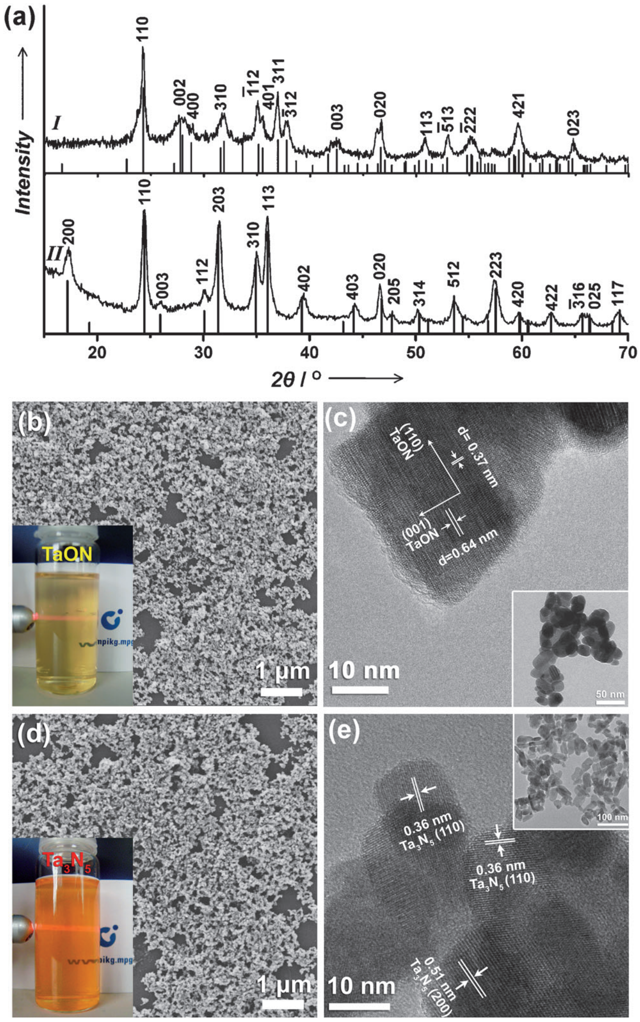

**Figure 1.** a) XRD patterns of I) TaON and II) $Ta_3N_5$ NPs obtained by the $SiO_2$-surface-assisted urea method with $R_{U/Ta}$ values of 1.5 and 3.0. The simulated patterns for γ-TaON and $Ta_3N_5$ are also shown. b) SEM and c) TEM images of TaON NPs, and d) SEM and e) TEM images of $Ta_3N_5$ NPs. Insets of (b) and (d) shows photos of TaON and $Ta_3N_5$ NPs dispersed in EtOH.

and $Ta_3N_5$ NPs in the presence of $SiO_2$. It was found that $SiO_2$ is indispensable. Without $SiO_2$, only bulky mixtures of TaON, $Ta_3N_5$, and even $Ta_4N_5$ were obtained, indicating that the controlled nitridation and nucleation relies on the large-surface $SiO_2$ template (Figure S3). Because of the easy overreactions during nitridation, mixtures of TaON and $Ta_3N_5$ were obtained with $R_{U/Ta}$ values ranging from 1.5 to 4.0 in the absence of silica. $Ta_3N_5$ becomes predominant when the $R_{U/Ta}$ value is increased to 6.0, but unfortunately it is accompanied by TaON and $Ta_4N_5$ as by-products. Further experiments reveal that the specific surface area of $SiO_2$ is significant to its function to avoid overreactions. When bulky $SiO_2$ (ca. 500 nm) with a small surface area of $S_{BET} = 5.6\ m^2\,g^{-1}$ was used, the overreactions could not be avoided, and only the mixture of TaON and $Ta_3N_5$ was received at $R_{U/Ta}$ values of 1.5 and 3.0, respectively (Figure S4). Therefore, the interactions and reactions between the $SiO_2$ surface and urea should be taken into account for the controlled generation of TaON and $Ta_3N_5$ NPs.

It is well known that upon fast heating from 300 to 420 °C, urea decomposes to ammonia and isocyanic acid [Eq. (1)].[8] Catalyzed by OH groups on silica, isocyanic acid is converted into cyanamide, which can trimerize to form melamine [Eqs. (2) and (3)].[8] The overall reaction is given in Equation (4).

$$(NH_2)_2CO \xrightarrow{300-420\,^\circ C} HNCO + NH_3 \qquad (1)$$

$$2\,O{=}C{=}N{-}H \xrightarrow[400\,^\circ C]{[SiO_2]-OH} H_2N{-}C{\equiv}N + CO_2 \qquad (2)$$

$$3\,H_2N{-}C{\equiv}N \xrightarrow{400\,^\circ C} C_3N_3(NH_2)_3 \qquad (3)$$

$$6(NH_2)_2CO \xrightarrow{400\,^\circ C/SiO_2} C_3N_3(NH_2)_3 + 6\,NH_3 + 3\,CO_2 \qquad (4)$$

With further thermal treatment, as-formed melamine polycondenses to $CN_x$ species with yellow melon and even s-triazines.[9] The formation of $CN_x$ species from urea during our calcination can be well confirmed by FTIR investigation. After treating TaU/SN precursor at 500 °C, the FTIR spectrum (Figure 2 a) clearly displays the characteristic bands associated with the vibrations of C≡N ($2053\ cm^{-1}$), C-N(-C)-C ($1363\ cm^{-1}$) and s-triazine (1624 and $1556\ cm^{-1}$).[8a,10] Similar observations for the process without $SiO_2$ suggest that the conversion from urea to $CN_x$ can be also achieved by Ta–OH. However, the above absorption bands in the presence of $SiO_2$ are blue-shifted relative to those without $SiO_2$, which implies that the interaction between the $SiO_2$ surface and $CN_x$ stabilizes the $CN_x$ species.[11] Moreover, the large surface area of $SiO_2$ NPs remarkably enhances such function. Because $CN_x$ is available for metal nitridation through decomposition to active N species,[12] its delayed decomposition on $SiO_2$ surface is significant for controlled nitridation. The different $CN_x$ decompositions against heating with and without $SiO_2$ can be well reflected by the evolution of N content in TaU/SN and TaU ($R_{U/Ta} = 3.0$) treated from 500 to 700 °C (Figure 2 b). $CN_x$ decomposition slows down with the assistance of $SiO_2$. The content of N is kept at the same level around 8.0 wt % under 650 °C, and remarkably decreases to 6.97 wt % at 700 °C, indicating major decomposition around 700 °C. However, without $SiO_2$, the N content is drastically and continuously decreased from 500 to 700 °C. The mole ratios of N/Ta also present the consistent evolution. It should be pointed out that the easier $CN_x$ decomposition in TaU will induce inhomogeneous N species atmosphere and consequent overreactions.[4] Thus, the formation and stabilization of $CN_x$ on large $SiO_2$ surface is important for TaON and $Ta_3N_5$ controlled synthesis because of the suppression of N source release (Figure 2 c).

In this mechanism, the surface area of silica is the key factor. If the same amount of mesoporous SBA-15 with larger surface ($S_{BET} = 675.4\ m^2\,g^{-1}$) than $SiO_2$ NPs is employed, pure TaON NPs are obtained at a lower $R_{U/Ta}$ value of 1.0 (Figure S6), which suggests that more $CN_x$ can be stored on the larger surface of SBA-15. When the $R_{U/Ta}$ ratio is increased to 4.0 and 5.0, the deep nitridation product, $Ta_4N_5$, is generated as a result of excessive $CN_x$ within SBA-15, compared with pure $Ta_3N_5$ NPs obtained at the same ratios using $SiO_2$ NPs (see Figure S2). This result further validates

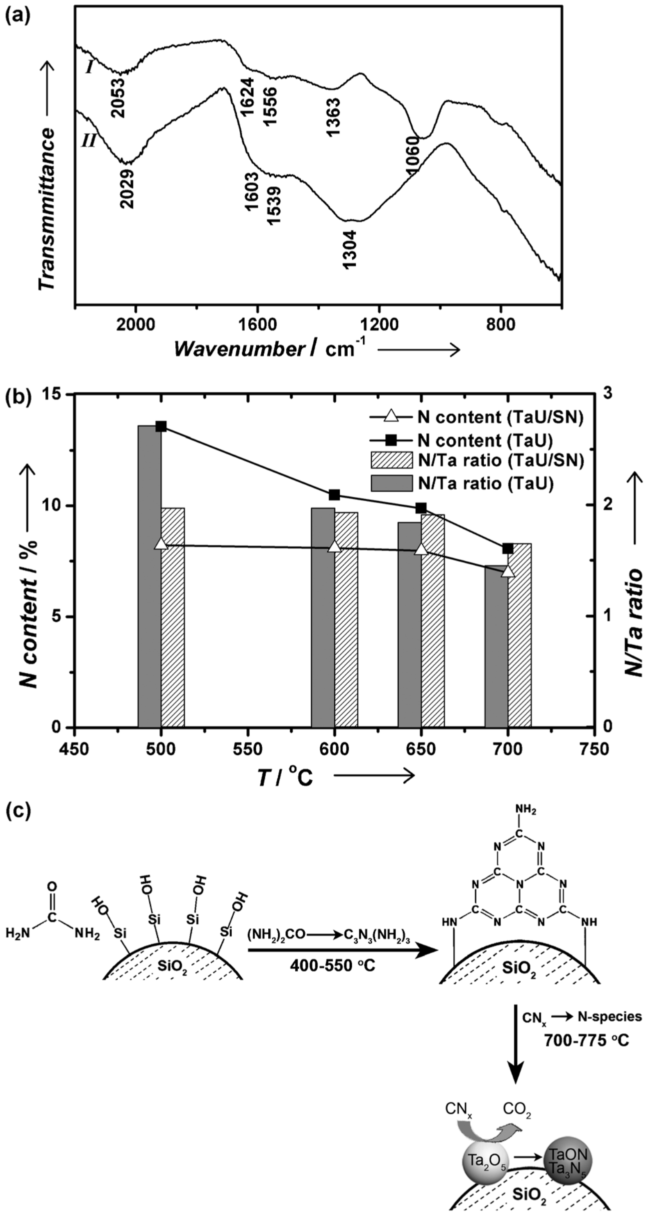

***Figure 2.*** a) FTIR spectra of products obtained after treating I) TaU/SN and II) TaU at 500 °C. b) N content and N/Ta mole ratio evolutions of TaU/SN and TaU with increasing temperatures. c) Illustration of $SiO_2$-surface-assisted mechanism for controllable synthesis of TaON and $Ta_3N_5$ NPs through $CN_x$-intermediate process catalyzed by $SiO_2$.

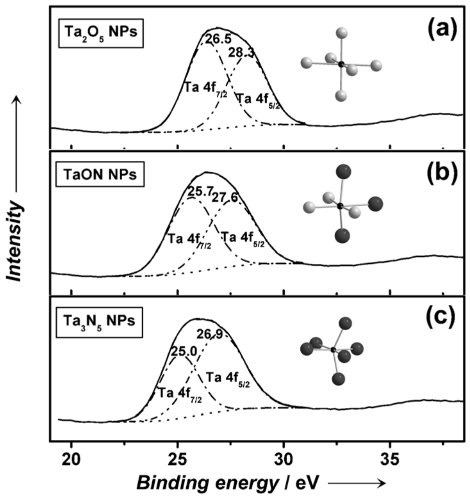

***Figure 3.*** Ta 4f XPS spectra of a) $Ta_2O_5$, b) TaON, and c) $Ta_3N_5$ NPs. The Ta 4f peaks are shifted to lower energies and have increased N/O ratio in TaON and $Ta_3N_5$ NPs relative to those of $Ta_2O_5$. The structures in the insets of (a–c) present the octahedral coordination environment of a) $Ta_2O_5$, b) TaON, and c) $Ta_3N_5$. Ta small black ball, O gray ball, N large black ball.

the mechanism of the $SiO_2$ surface for achieving controlled nitridation. Additionally, such a mechanism was also found to be general for other metals such as Zr, in which $Zr_2N_2O$ NPs are well obtained and overreaction ZrN is suppressed by $SiO_2$ (Figure S7). We believe this will open up opportunities to design various nanostructures of functional metal–nitrides.

Changing the nitridation level of tantalum (oxy)nitrides provides a new approach to tune the electronic properties of Ta atom, because of the lower electronegativity of N atoms than O atoms. This situation is already indicated by X-ray photoelectron spectroscopy (XPS, Figure 3). In $Ta_2O_5$ NPs, the Ta $4f_{7/2}$ and $4f_{5/2}$ peaks appear at 26.5 and 28.3 eV (Figure 3a), which correspond to $Ta^{5+}$ in $Ta_2O_5$.[13] With the introduction of N, these peaks are shifted to lower binding energies of 25.7 and 27.6 eV in TaON, and 25.0 and 26.9 eV in $Ta_3N_5$, respectively (Figure 3b,c). The noticeable red shifts of about 0.8 and 1.5 eV in respective TaON and $Ta_3N_5$ are believed to be due to the easier electron transfer from N than O.[3a] Remarkably, the increased electron density around Ta will endow such nanoparticles with improved catalytic properties.

The oxides of group V are promising alkene oxidation catalysts,[14] and available Ta catalysts for epoxidation have recently attracted much attention because epoxides are important intermediates in fine chemical production and polymer synthesis.[15] Herein, we employed cyclooctene epoxidation as a probe reaction for our TaON and $Ta_3N_5$ NPs, as well as $Ta_2O_5$ NPs (Table 1). All of these NPs possess similar sizes (ca. 20 nm) and surface areas (ca. $20\,m^2\,g^{-1}$, Table S1). $Ta_2O_5$ NPs exhibit a low conversion of 57.1 %, whereas, improved activity with higher conversion of 96.0 % and 96.5 % was presented on TaON and $Ta_3N_5$ NPs, respectively (Table 1, entries 1–3). In view of their similar surface area, the improved activity of Ta in TaON and $Ta_3N_5$ should be ascribed to the increased electron density around Ta resulting from N introduction, as ascertained by XPS results in Figure 3. As reported, the epoxidation activity of Ta is associated with the step of [Ta·O*] reacting with alkene to epoxides, and can be improved by effective electron-donor ligands around Ta.[15c,d] In TaON and $Ta_3N_5$ NPs, the N atom can serve as an electron donor and promotes the O* transfer from [Ta·O*] to cyclooctene, consequently improving the activity (Step I in Scheme 1). According to XPS results, $Ta_3N_5$ NPs with lower Ta 4f binding energies than TaON is expected to be more active, and, correspondingly, its conversion of 65.4 % is observed to be higher than that on the latter (59.1 %) when reaction time is shortened (Table 1, entries 4 and 5). Furthermore, the epoxidation selectivity is also

***Table 1:*** Epoxidation of cyclooctene over $Ta_2O_5$, TaON, and $Ta_3N_5$ NPs[a].

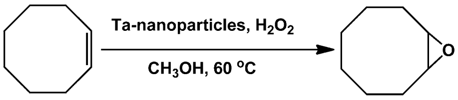

| Entry | Catalyst | Conversion [%] | Selectivity [%] |
|---|---|---|---|
| 1 | $Ta_2O_5$[b] | 57.1 | 95.9 |
| 2 | TaON[c] | 96.0 | 95.6 |
| 3 | $Ta_3N_5$[c] | 96.5 | 78.4 |
| 4 | TaON[d] | 59.1 | 97.9 |
| 5 | $Ta_3N_5$[d] | 65.4 | 79.8 |
| 6 | $Ta_3N_5$–H[e] | 96.9 | 85.8 |
| 7 | $Ta_2O_5$-H[e] | 57.9 | 97.9 |
| 8 | $Ta_2O_5$–OH[f] | 54.9 | 99.3 |
| 9 | TaON[g] | 96.8 | 96.1 |
| 10 | $Ta_3N_5$[g] | 99.0 | 85.4 |
| 11 | $Ta_3N_5$–OH[h] | 97.5 | 74.9 |
| 12 | blank | 12.8 | 99.0 |

[a] Typical reaction conditions: 0.92 mL of cyclooctene, 0.04 g of catalyst, 4.0 mL $CH_3OH$, and 3.0 mL $H_2O_2$ (50 wt%), 60 °C for 18 h. [b] $Ta_2O_5$ NPs were obtained through traditional reverse homogeneous precipitation (Figure S8). [c] TaON and $Ta_3N_5$ NPs were obtained by the $SiO_2$-surface assisted method. [d] The reaction time was decreased to 10 h. [e] Catalysts were used after treating with 1 M HCl for 1 day. [f] Catalyst was used after treating with 1 M $NH_3 \cdot H_2O$ for 1 day. [g] TaON and $Ta_3N_5$ NPs were obtained by Ca-assisted urea method. [h] $Ta_3N_5$ NPs obtained through Ca-assisted urea method were used after treating with 1 M $NH_3 \cdot H_2O$ for 1 day.

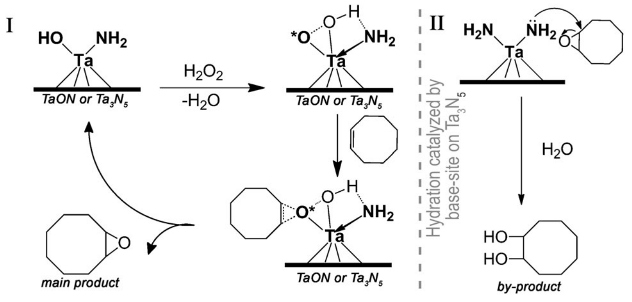

***Scheme 1.*** I) Epoxidation of cyclooctene by TaON and $Ta_3N_5$ NPs, and II) overreaction of hydration to diol products catalyzed by the basic site on $Ta_3N_5$.

significantly influenced by N introduction. $Ta_2O_5$ and TaON NPs present the selectivity as high as 95.9% and 95.6%, respectively, whereas only a lower selectivity of 78.4% is found on $Ta_3N_5$ (Table 1, entries 1–3). In the GC–MS results of products catalyzed by $Ta_3N_5$ NPs, considerable amounts (ca. 21.3%) of cyclooctane–(di)ol are detected (Figure S9), indicating the hydration of epoxide to (di)ol products as overreactions.[16] As enough N is introduced, a strong basic site will be generated on the catalysts,[17] such as $Ta_3N_5$, which is validated by their temperature programmed desorption (TPD) curves of $CO_2$ (Figure S10). Thus, catalyzed by base sites on $Ta_3N_5$ NPs, the as-formed epoxide is hydrated with water from $H_2O_2$ solution, resulting in decreased epoxide selectivity (Step II in Scheme 1). Moreover, such basicity originating from N is tunable by acid or base treatment because of reversible protonation, generating an altered selectivity. For example, the $Ta_3N_5$ NPs treated by 1 M HCl show the increased selectivity of up to 85.8% (Table 1, entry 6). Conversely, the selectivity on $Ta_2O_5$ NPs cannot be obviously varied by acid or base treatment (Table 1, entries 7 and 8), supporting again the surface base character derived from N atom.

The consistent performances of TaON and $Ta_3N_5$ NPs obtained by another Ca-assisted urea method[7] (Table 1, entries 9–11) further confirm the improved activity and tunable selectivity significantly associated with their tailored nitridation level. It should be noted that $Ta_3N_5$ NPs from Ca-assisted processes are received after HCl washing to remove Ca species, and they deliver epoxide selectivity of as high as 85.4%, which can be decreased to 74.9% after treating with 1 M $NH_3 \cdot H_2O$ (Table 1, entry 11). From the above results, it can be concluded that introducing N significantly promotes the Ta activity for epoxidation, and also generates tunable basicity important to tailor the epoxide selectivity. Controlled nitridation plays a key role in epoxidation, and, herein, TaON NPs with suitable nitridation degree present high activity and selectivity.

In summary, a novel $SiO_2$-surface-assisted urea method was introduced for the controlled synthesis of TaON and $Ta_3N_5$ NPs. By varying the urea/Ta ratio in the precursor gel, both TaON and $Ta_3N_5$ NPs with defined structure and size can be achieved. Moreover, a novel mechanism employing $SiO_2$ surfaces is proposed whereby silica catalyzes and stabilizes $CN_x$ formation to achieve a slow release N source for controlled nitridation. The as-synthesized TaON and $Ta_3N_5$ NPs show improved activity and tunable selectivity for cyclooctene epoxidation. This behavior is explained by the increased electron density around Ta and surface basicity based upon the controlled introduction of N atom. The nitridation level is important to achieve highly active and selective metal catalysts for epoxidation, and our method is believed to be broadly applicable to the design of novel nanostructured catalysts.

Received: October 12, 2011

**Keywords:** epoxidation · nanoparticles · surface chemistry · tantalum

---

[1] a) N. E. Breese in *Structure and Bonding, Crystal Chemistry of Inorganic Nitride*, Springer, Berlin, **1992**; b) H. Morkoc, S. N. Mohammad, *Science* **1995**, *267*, 51; c) E. Gregoryanz, C. Sanloup, M. Somayazulu, J. Badro, G. Fiquet, H. K. Mao, R. J. Hemley, *Nat. Mater.* **2004**, *3*, 294; d) A. M. Alexander, J. S. J. Hargreaves, *Chem. Soc. Rev.* **2010**, *39*, 4388; e) M. H. Yang, J. Oro-Sole, J. A. Rodgers, A. B. Jorge, A. Fuertes, J. P. Attfield, *Nat. Chem.* **2011**, *3*, 47; f) Q. S. Gao, C. X. Zhang, S. H. Xie, W. M. Hua, Y. H. Zhang, N. Ren, H. L. Xu, Y. Tang, *Chem. Mater.* **2009**, *21*, 5560.
[2] a) K. Maeda, K. Domen, *J. Phys. Chem. C* **2007**, *111*, 7851; b) R. Abe, M. Higashi, K. Domen, *J. Am. Chem. Soc.* **2010**, *132*, 11828; c) X. J. Feng, T. J. LaTempa, J. I. Basham, G. K. Mor, O. K. Varghese, C. A. Grimes, *Nano Lett.* **2010**, *10*, 948; d) S. Ito, K. R. Thampi, P. Comte, P. Liska, M. Gratzel, *Chem. Commun.* **2005**,

268; e) M. Hara, G. Hitoki, T. Takata, J. N. Kondo, H. Kobayashi, K. Domen, *Catal. Today* **2003**, *78*, 555.

[3] a) W. J. Chun, A. Ishikawa, H. Fujisawa, T. Takata, J. N. Kondo, M. Hara, M. Kawai, Y. Matsumoto, K. Domen, *J. Phys. Chem. B* **2003**, *107*, 1798; b) R. Asahi, T. Morikawa, T. Ohwaki, K. Aoki, Y. Taga, *Science* **2001**, *293*, 269; c) C. Di Valentin, G. Pacchioni, A. Selloni, *Phys. Rev. B* **2004**, *70*, 085116.

[4] a) E. Orhan, F. Tessier, R. Marchand, *Solid State Sci.* **2002**, *4*, 1071; b) M. Kerlau, O. Merdrignac-Conanec, M. Guilloux-Viry, A. Perrin, *Solid State Sci.* **2004**, *6*, 101.

[5] a) G. Brauer, J. R. Weidlein, *Angew. Chem.* **1965**, *77*, 867; *Angew. Chem. Int. Ed. Engl.* **1965**, *4*, 875; b) G. Brauer, J. R. Weidlein, *Angew. Chem.* **1965**, *77*, 218; *Angew. Chem. Int. Ed. Engl.* **1965**, *4*, 241; c) H. Schilling, A. Stork, E. Irran, H. Wolff, T. Bredow, R. Dronskowski, M. Lerch, *Angew. Chem.* **2007**, *119*, 2989; *Angew. Chem. Int. Ed.* **2007**, *46*, 2931.

[6] a) J. Buha, I. Djerdj, M. Antonietti, M. Niederberger, *Chem. Mater.* **2007**, *19*, 3499; b) H. Z. Zhao, M. Lei, X. L. Chen, W. H. Tang, *J. Mater. Chem.* **2006**, *16*, 4407.

[7] Q. S. Gao, C. Giordano, M. Antonietti, *Small* **2011**, *7*, 3334.

[8] a) D. Mitoraj, H. Kisch, *Chem. Eur. J.* **2010**, *16*, 261; b) A. Schmidt, *Chem. Ing. Tech.* **1966**, *38*, 1140.

[9] a) X. C. Wang, K. Maeda, A. Thomas, K. Takanabe, G. Xin, J. M. Carlsson, K. Domen, M. Antonietti, *Nat. Mater.* **2009**, *8*, 76; b) X. C. Wang, K. Maeda, X. F. Chen, K. Takanabe, K. Domen, Y. D. Hou, X. Z. Fu, M. Antonietti, *J. Am. Chem. Soc.* **2009**, *131*, 1680.

[10] a) B. Jürgens, E. Irran, J. Senker, P. Kroll, H. Muller, W. Schnick, *J. Am. Chem. Soc.* **2003**, *125*, 10288; b) T. Komatsu, *Macromol. Chem. Phys.* **2001**, *202*, 19; c) B. V. Lotsch, M. Doblinger, J. Sehnert, L. Seyfarth, J. Senker, O. Oeckler, W. Schnick, *Chem. Eur. J.* **2007**, *13*, 4969.

[11] Q. S. Gao, P. Chen, Y. H. Zhang, Y. Tang, *Adv. Mater.* **2008**, *20*, 1837.

[12] a) A. Fischer, M. Antonietti, A. Thomas, *Adv. Mater.* **2007**, *19*, 264; b) A. Fischer, J. O. Muller, M. Antonietti, A. Thomas, *ACS Nano* **2008**, *2*, 2489; c) J. Chen, K. Takanabe, R. Ohnishi, D. L. Lu, S. Okada, H. Hatasawa, H. Morioka, M. Antonietti, J. Kubota, K. Domen, *Chem. Commun.* **2010**, *46*, 7492.

[13] O. Kerrec, D. Devilliers, H. Groult, P. Marcus, *Mater. Sci. Eng. B* **1998**, *55*, 134.

[14] a) R. L. Brutchey, C. G. Lugmair, L. O. Schebaum, T. D. Tilley, *J. Catal.* **2005**, *229*, 72; b) D. Meunier, A. Piechaczyk, A. de Mallmann, J. M. Basset, *Angew. Chem.* **1999**, *111*, 3738; *Angew. Chem. Int. Ed.* **1999**, *38*, 3540; c) I. Nowak, B. Kilos, M. Ziolek, A. Lewandowska, *Catal. Today* **2003**, *78*, 487.

[15] a) P. J. Cordeiro, T. D. Tilley, *Langmuir* **2011**, *27*, 6295; b) N. Morlanés, J. M. Notestein, *J. Catal.* **2010**, *275*, 191; c) D. A. Ruddy, T. D. Tilley, *Chem. Commun.* **2007**, 3350; d) D. A. Ruddy, T. D. Tilley, *J. Am. Chem. Soc.* **2008**, *130*, 11088.

[16] a) Z. J. Yang, N. Ren, Y. H. Zhang, Y. Tang, *Catal. Commun.* **2010**, *11*, 447; b) M. Guidotti, C. Pirovano, N. Ravasio, B. Lazaro, J. M. Fraile, J. A. Mayoral, B. Coq, A. Galarneau, *Green Chem.* **2009**, *11*, 1421.

[17] a) H. Li, Q. Lei, X. M. Zhang, J. H. Suo, *ChemCatChem* **2011**, *3*, 143; b) Y. D. Xia, R. Mokaya, *J. Phys. Chem. C* **2008**, *112*, 1455.